Meas. Sci. Technol. **20** (2009) 015802 (9pp) doi:10.1088/0957-0233/20/1/015802

System automation for a bacterial colony detection and identification instrument via forward scattering

Euiwon Bae[1], Amornrat Aroonnual[2], Arun K Bhunia[2], J Paul Robinson[3] and E Daniel Hirleman[1]

[1] School of Mechanical Engineering, Purdue University, West Lafayette, IN 47906, USA
[2] Molecular Food Microbiology Laboratory, Department of Food Science, Purdue University, West Lafayette, IN 47906, USA
[3] Department of Basic Medical Science, Weldon School of Biomedical Engineering, Purdue University, West Lafayette, IN 47906, USA

Received 30 July 2008
Published 12 November 2008
Online at stacks.iop.org/MST/20/015802

Abstract
A system design and automation of a microbiological instrument that locates bacterial colonies and captures the forward-scattering signatures are presented. The proposed instrument integrates three major components: a colony locator, a forward scatterometer and a motion controller. The colony locator utilizes an off-axis light source to illuminate a Petri dish and an IEEE1394 camera to capture the diffusively scattered light to provide the number of bacterial colonies and two-dimensional coordinate information of the bacterial colonies with the help of a segmentation algorithm with region-growing. Then the Petri dish is automatically aligned with the respective centroid coordinate with a trajectory optimization method, such as the Traveling Salesman Algorithm. The forward scatterometer automatically computes the scattered laser beam from a monochromatic image sensor via quadrant intensity balancing and quantitatively determines the centeredness of the forward-scattering pattern. The final scattering signatures are stored to be analyzed to provide rapid identification and classification of the bacterial samples.

Keywords: bacterial colony, forward scattering, automation

1. Introduction

Bacterial contamination in food, water and other sources is monitored through a standard laboratory practice of counting the number of colonies (colony-forming units, CFU) formed on a solid growth medium in a Petri dish. In recent years, the counting efficiency of cells or bacterial colonies has been improved through various computerized image processing schemes. Previous researches applied the distance transforms [1], multiple/adaptive thresholds [2], the fuzzy method [3], a predefined intensity model [4] and the modified Hough transform [5] to enhance the sensitivities of the image processing schemes. However, previous researches were mostly concentrated on counting the cells or bacterial colonies and additional steps, such as serotyping, morphological analysis and proteomics/genomics, are still required to identify and classify the bacterial colonies present in a sample. Among these, morphological methods observe the morphological characteristics of the bacterial colony via visual inspection which could be differentiated when there are substantially different macroscopic features, such as shape, thickness or color [6–8]. However, an interrogating source (i.e. a laser source) is capable of analyzing and extracting the microscopic morphological differences even when different types of bacterial colonies are visually indistinguishable. Recent studies conducted by Guo [9] and Banada [10] demonstrated the possibility of using a transmission and reflection type of the bacterial colony scattering method for a rapid, label-free detection of the pathogenic bacteria. They also suggested the feasibility of using the transmission type (forward scattering) for the bacterial colony detection/identification. Based on these

results, the forward scatterometer was upgraded with improved designs and named the bacterial rapid detection using optical scattering technology (BARDOT). Bio-physical reasons for different forward-scattering patterns were analyzed via phase contrast/confocal microscopy and the scalar diffraction theory successfully regenerated the forward-scattering pattern by modeling the bacterial colonies as an amplitude/phase modulator [11]. In addition, the time dependence of the bacterial colony growth versus the forward-scattering pattern was also analyzed for three species of *Listeria* [12]. Although the captured forward-scattering patterns were distinctive among tested species, a quantitative method for discriminating the forward-scattering pattern was proposed via applying Zernike moment invariants due to the rotational symmetry of the scattering pattern. Detailed derivation and application of the captured scattering pattern was reported in reference [13].

The current BARDOT system requires a human operator to position the bacterial colony to the incident laser beam and adjust it such that the forward-scattering patterns are rotationally symmetric. This task is an iterative process and requires constant attention and time of an operator which requests the development of automation that will increase the efficiency and reduce the time for the bacterial identification. Here, we suggest system automation of a microbiological instrument that not only counts and locates the bacterial colonies but also automatically measures the forward-scattering signature to identify the species of the bacterial colony under investigation without the need to use other molecular- or biosensor-based detection methods [14]. The proposed instrument could be manufactured for a routine bacterial detection and identification tool in microbiology laboratories.

Section 2 discusses the material and methods, such as sample preparation, hardware and software parts of the system. Section 3 provides the experimental result of the actual measurement performed on bacterial colonies in a Petri dish. Section 4 discusses the effectiveness and the quantitative result from two types of image sensors.

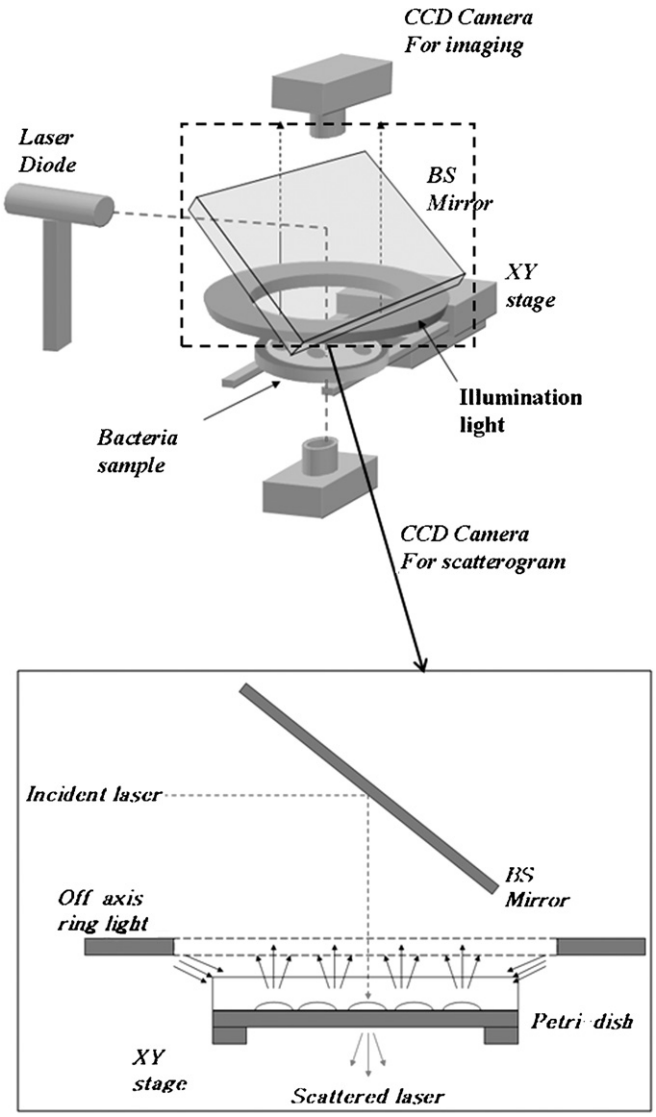

Figure 1. Schematic diagram of automatic BARDOT (bacterial rapid detection using optical scattering technology) platform with two CCD image sensors.

2. Material and methods

2.1. Sample preparation

Listeria innocua F4248 culture is selected for our experiments. A single colony from brain heart infusion (BHI) agar is transferred and grown in BHI broth at 37± °C for 15–18 h. Bacterial culture is then 10-fold serially diluted in phosphate buffer saline (PBS) pH 7.2 and dilutions are plated on the surface of BHI agar in a Petri dish, so as to obtain 10–30 colonies per plate and are incubated at 37 °C. The plates are incubated for 30–42 h until the diameter of the bacterial colonies reaches approximately 1.3 ± 0.2 mm.

2.2. Hardware

As shown in figure 1, the automated BARDOT system consists of the following three major components: a colony locator, a forward scatterometer and a two-dimensional motorized stage. The colony locator part is composed of an IEEE-1394 RGB camera (Unibrain Inc., San Ramon, CA, USA) with $f = 4.3$ lens and viewing angles of 42° and 32° in the horizontal (H) and vertical (V) directions, respectively. Illumination is provided by a 20 W off-axis fluorescent ring light source (Osram, PA, USA). The colony locator camera has 640 (H) × 480 (V) resolution and a unit pixel size of 5.6 × 5.6 μm^2. The difference between previous colony counters [1–5] and the automatic BARDOT is that another laser source has to pass through the Petri dish such that the forward-scattering signature is created and captured. Previous research intentionally employed a black background to improve contrast of the bacterial colony to the background [4], while in the automatic BARDOT system we apply spatial filtering to isolate the Petri dish and a gray scale threshold to isolate the bacterial colonies. The off-axis fluorescent ring light has 6 inch of clear aperture to illuminate the Petri dish

from the side. The selection of the off-axis fluorescent light is a design decision to provide simultaneous illumination of the bacterial colonies and capturing of the forward-scattering pattern. Compared with other light sources used in previous research such as a strobe light or a diffuse dome light, an off-axis ring light provides a clear aperture with a relatively constant illumination over the inspected area, eliminates the specular reflection from the agar surface and the cover of the Petri dish and requires small space to fit into the optical system.

The forward-scattering part is composed of a laser diode module of 635 nm wavelength (Coherent Inc., Santa Clara, CA, USA) which is selected on the longer end of the visible wavelength since short-*wavelength* radiation (i.e. UV) tends to affect the biological samples. For the imaging sensor, a monochromatic IEEE-1394 CCD image sensor (MicroPix, London, UK) with 640 × 480 resolution and 7.4 × 7.4 μm^2 unit pixel size is positioned under the Petri dish at a distance of 30 mm from the bottom of the Petri dish to the surface of the CCD image sensor. The plate beam splitter (BS) with a thickness of 3 mm (Edmund Optics, NJ, USA) is placed on top of the Petri dish such that 70% of backscattered light is transmitted to the imaging camera while 30% of diode laser power is directed to the sample. This plate BS is coated with antireflection coating so that only a single incident laser beam is directed to the bacterial colony and forward-scatterometer camera. The plate BS reflects images of four sides which increase the background noise to the bacterial colony locator camera and render the image processing more complicated; we build an enclosure to reduce the reflection images from the left and right sides of the BS and provided 10 × 10 mm square aperture on the left side of the enclosure for the incident laser to pass through.

The motion control part consists of two linear motors (850G-HS) connected to the ESP300 multi-axis closed-loop controller (Newport, NY, USA). The specification of the linear motor has a 42 mm maximum stroke, a minimum step size of 0.1 μm and a speed of 5 mm s^{-1}. The ESP300 controller is connected to a PC (Pentium 3 GHz with 2 Gb RAM) with a serial port and controlled by a graphical user interface written with the Visual C++ 6.0 software (Microsoft, Seattle, WA, USA).

2.3. Software

The software part also consists of three parts. As shown in figure 2, the automatic BARDOT system acquires the sample information and aligns the sample with the incident laser until the last scattering signature of the bacterial colonies is captured. For the colony locating part, a Visual C++ program is written to count and locate the center of the bacterial colonies. This is realized by first spatially filtering the outside of the Petri dish and filling these areas with all LOW (0) values. Then, we designate an 8 bit pixel intensity value of the bacterial colony as a HIGH value which is higher than 235 and filter out the rest of the background. The segmentation and counting of the bacterial colony is performed by the well-known algorithm of the segmentation with region-growing [15–17]. The algorithm loops through the image array looking for a HIGH value.

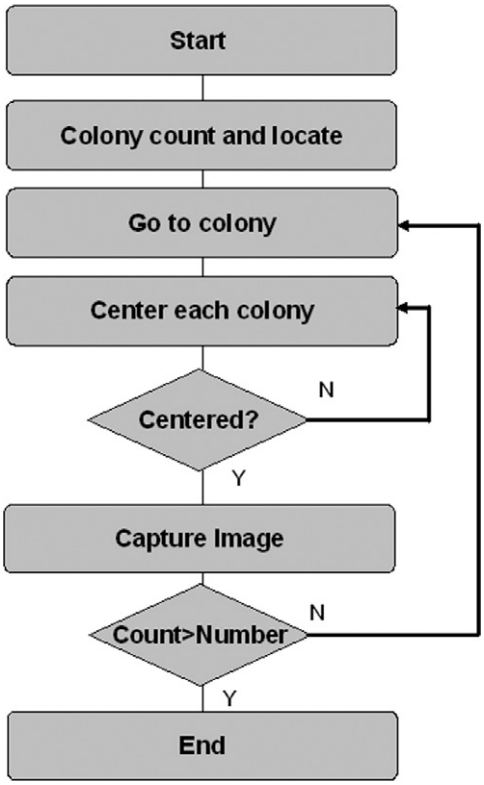

Figure 2. Flow chart for operating procedure for the automatic BARDOT system.

When it finds a HIGH pixel, it assigns a colony count value and checks the pixel's eight neighbor points to see if there is a HIGH pixel. After the surrounding HIGH pixels are located and filled with colony count value, the algorithm searches the next cluster to repeat the process. Each step increases the region-growing counter and the last number provides the total number of colonies found. Next step is to compute the two-dimensional center location of individual colonies. This is realized via computing the two-dimensional centroid from the binarized image.

After the bacterial colonies are counted and located, there is an issue of optimizing the traveling sequence through all identified colony locations. The two-dimensional loop of the Visual C++ code shows a horizontal (640 pixel) and a vertical (480 pixel) scan. Therefore, the region-growing algorithm assigns a region number whenever it finds a cluster starting from the bottom-left corner. Therefore, the natural numbering sequence follows the scanning loop and the total traveling trajectory may include numerous redundant trajectories which are not optimized for fast and efficient traveling. This is the so-called Traveling Salesman Problem (TSP) which is to find the route that minimizes the total travel length while visiting each location only once. Here, we tested the TSP algorithm with cross entropy (CE) and genetic algorithm (GA) methods assuming there are n colonies to travel. For the CE method, once the centroid of each cluster is computed, we create a cost matrix for 1 to nth colony which has the travel length from ith colony to the adjacent node and compute the trajectory that minimizes the entropy of all possible traveling routes [18–20]. For the GA method, we define the same cost matrix as the CE

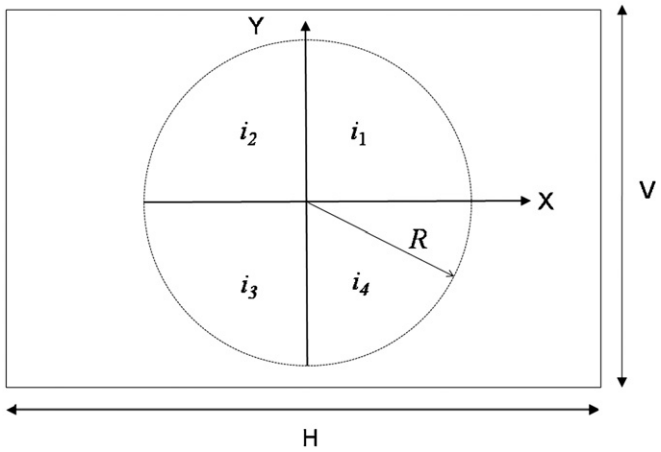

Figure 3. The schematic diagram of the definition of QIB of a CCD camera for forward scattering. The diagram displays the 640 (H) × 480 (V) CCD imaging area with the *XY*-coordinate axis along with the dynamic radius *R* which is determined via a threshold value of background noise values. i_1 to i_4 denote the sensor quadrant where all the incoming scattering signal is summed.

method and select the two shortest sequences for a set of parent sequences. Then, we combine them to create two new child tour sequences and a certain ratio of tour sequence is mutated to prevent identical sequences. This new child sequence is inserted into the two longer tours and this step is repeated until the maximum iterations [21–23].

The software for the forward-scattering part is to calculate the intensity balance of the scattering image and center the forward-scattering image such that it can be processed through the classification algorithm [13]. Although typical forward-scattering patterns are rotationally symmetric, randomness of the colony morphology creates non-symmetric patterns (i.e. speckle patterns) in some species [11, 12]. Therefore to effectively automate the centering process of various types of forward-scattering pattern, we define a quantity called quadrant intensity balancing (QIB) for the *X*- and *Y*-directions which is defined as

$$\mathrm{QIB}_x = \frac{(i_1 + i_4) - (i_2 + i_3)}{i_1 + i_2 + i_3 + i_4}, \tag{1}$$

$$\mathrm{QIB}_y = \frac{(i_1 + i_2) - (i_3 + i_3)}{i_1 + i_2 + i_3 + i_4}, \tag{2}$$

where i_1 to i_4 are the total intensity from each quadrant centered on the imaging frame as shown in figure 3. The centeredness of the scattered laser beam is computed via balancing the total photons in each quadrant. The QIB radius, *R*, is calculated by the maximum pixel distance from the frame center that is higher than the background noise value which is approximately 60 in our experiment. Based on the output of the QIB, the system automatically adjusts the displacement such that the incident laser beam is centered on a single bacterial colony. Since the bacterial colony might not be perfectly symmetric and the measured 2D centroidal location is not identical to the scattering center, 2D fine adjustment is required for the quality of the forward-scattering image.

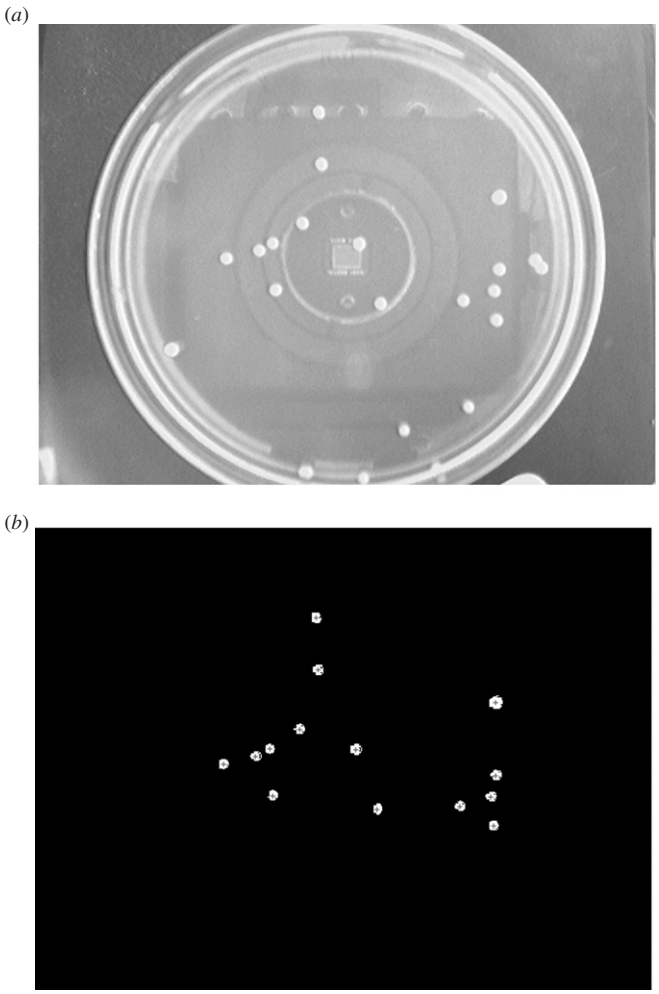

Figure 4. The result of applying the image processing method on *Listeria* colonies. The upper image (*a*) shows the raw image while the bottom image (*b*) shows the result of the region-growing with segmentation.

The aim of the motion controlling software is to position the *XY* stage to the desired position such that the forward-scattering signature is centered on the imaging sensor. The coordinate information of a certain bacterial colony is transferred from the colony locating software and the stage controller moves to the approximate location for each colony center (coarse movement). Then, communicating with forward-scattering software via QIB, the *XY* stage adjusts the position such that the forward-scattering image is centered (fine movement).

3. Experimental result

3.1. Colony locating

Figure 4 shows the result of the segmentation via a region-growing algorithm. Figure 4(*a*) shows the output from the imaging camera which shows the forward-scattering camera, the Petri dish and the stage system. Figure 4(*b*) displays the result of segmentation with a region-growing algorithm which shows the isolated clusters inside the Petri-dish diameter. The

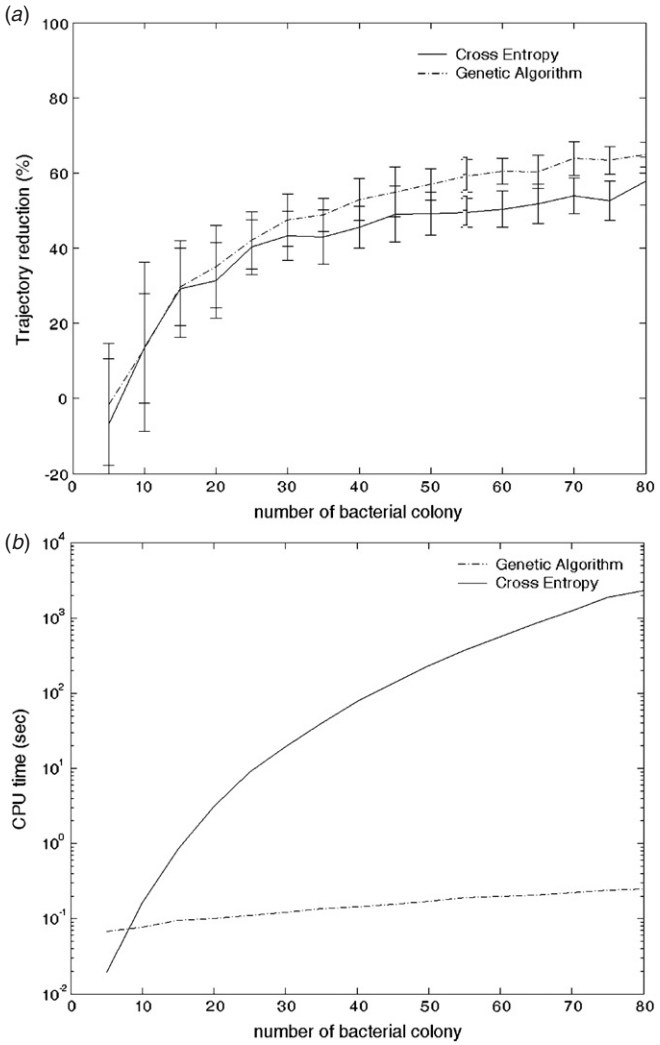

Figure 5. Simulation result of two algorithms for a trajectory optimization of various number densities of bacterial colonies and respective CPU times. The figure shows that for both GA and CE algorithms, the trajectory optimization efficiency increases when the number densities of bacterial colonies increase while the efficiency tends to saturate. For the CPU time required to solve the algorithm, GA solved the same optimization problem much faster than the CE algorithm.

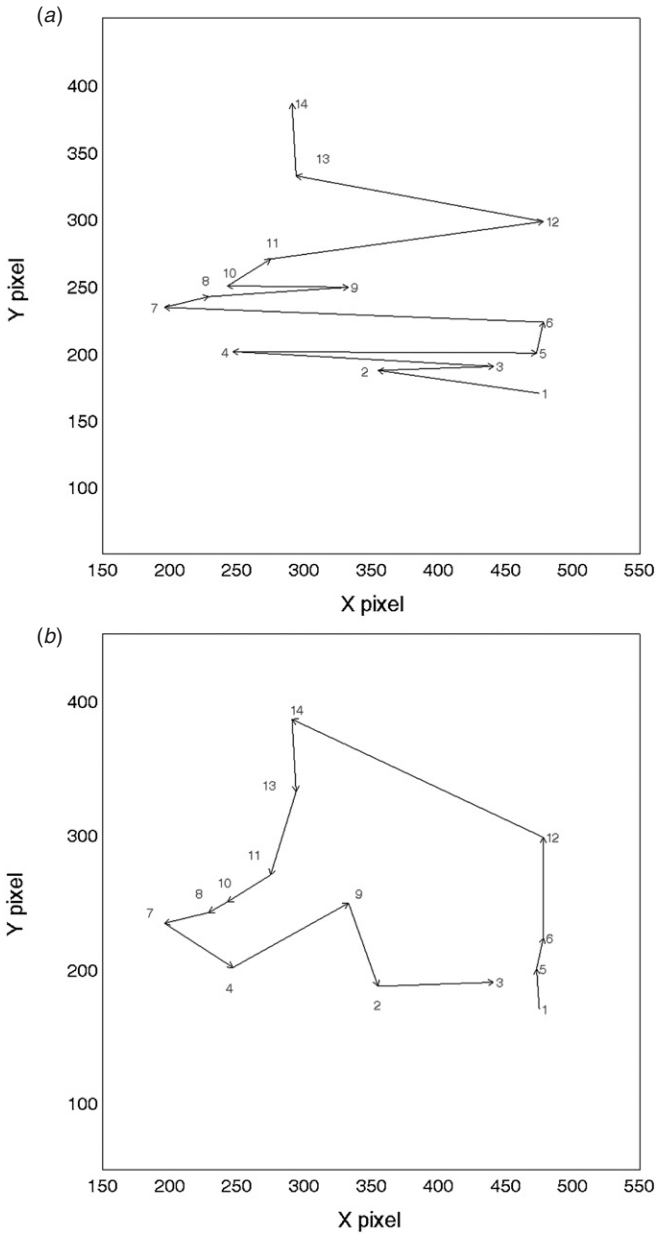

Figure 6. Comparison of (*a*) non-optimized and (*b*) optimized traveling orders of 14 colonies. The non-optimized case has a total travel length of 1780 pixels while the optimized case showed 1092 pixels. The optimized case is originated from the Traveling Salesman Problem with the GA method.

calculated centroid of each cluster is shown with a cross at the computed locations. Due to the physical limitation of the stroke of Newport 850G-HS, we limited our interrogation region to 40 mm × 40 mm square regions of the center of the Petri dish. Furthermore, in forward-scattering measurement, we excluded the bacterial colonies growing on the edge of the Petri dish since they do not grow in a flat agar area which distorts the forward-scattering pattern significantly.

To investigate the situation of trajectory optimization for the bacterial colony detection, we simulate different bacterial colony densities and their relationship to optimization efficiency and computational overhead. The bacterial density is varied from 5 to 80 colonies with the increment of 5 colonies on a 400 × 400 pixel domain with random distribution. Then both TSP algorithms are performed on each bacterial colony distribution and computed the optimization efficiently along with the computational time required to solve the TSP algorithm. On each distribution, the simulation is repeated with different random distributions 20 times to provide statistical results. Computational parameters for each method are presented in tables 1 and 2. Figure 5 shows the result of the optimization efficiency and the CPU time required for the GA and CE methods. The trajectory optimization efficiency, T_e, is defined as

$$T_e = \frac{(T_{N\,opt} - T_{opt})}{T_{N\,opt}} \times 100, \tag{3}$$

where T_{Nopt} and T_{opt} represent the total trajectory length of the non-optimized and optimized cases, respectively. According

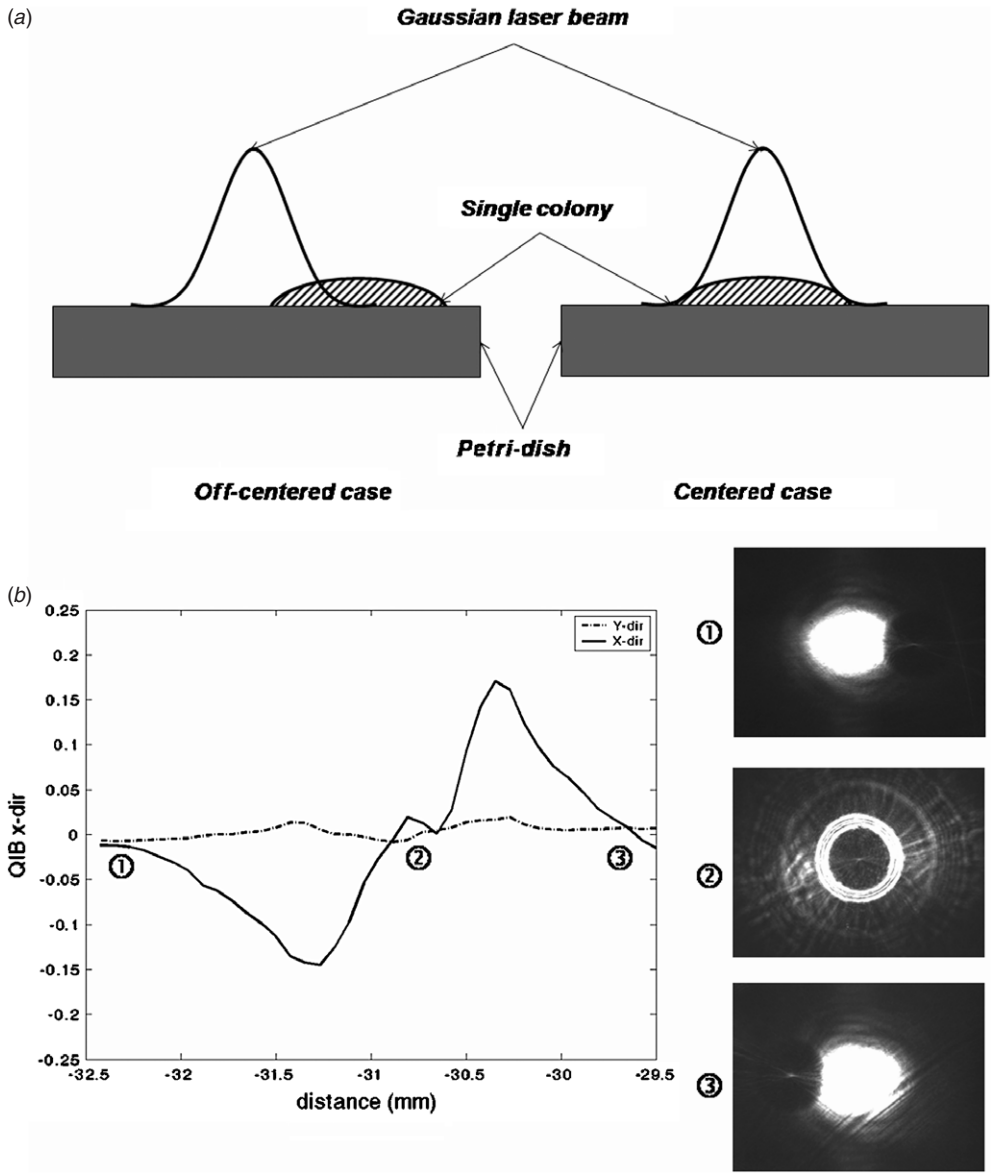

Figure 7. Relationship of quadrant intensity balancing (QIB) when the *L. innocua* colony is moved across the incident beam. (*a*) The centeredness of the incident laser beam and the single bacterial colony. In (*b*), images (1) and (3) denote when the colony barely hits the edge of the incident beam while image (2) shows the scattering pattern when the colony is centered on the incident beam.

Table 1. Computation parameters for the GA method.

Parameter	Symbol	Value
Number of iterations	N	500
Sample size	s	100
Mutate rate	μ	0.8

Table 2. Computation parameters for the CE method.

Parameter	Symbol	Value
Number of samples for each round	N	500
Fraction of best samples	ρ	0.05
Smoothing parameter	μ	0.8
Tolerance	τ	0.005

to the result, T_e increases as the number of bacterial colony distribution increases while T_e does not improve beyond 60% as shown in figure 5(*a*). However, this result comes with the price of CPU time to solve the TSP problem. According to figure 5(*b*), the CPU time for the CE method increases dramatically when the number of colonies is large while the GA only required 0.145 s to solve the optimal trajectory of the 80 bacterial colony distributions.

Figure 6 shows a comparison of the traveling sequence of 14 bacterial colonies of figure 4 for the non-optimized and optimized cases. The non-optimized case of figure 6(*a*) assigns the sequence from the origin (bottom-left corner). If the system follows this sequence, the path shows a 'zig-zag' motion which has a total traveling length of 1780 pixels, while the optimized case of figure 6(*b*) with the GA and CE methods shows that of 1092 pixels, which is 37% reduction in the total travel length with 0.048 and 0.85 s CPU times.

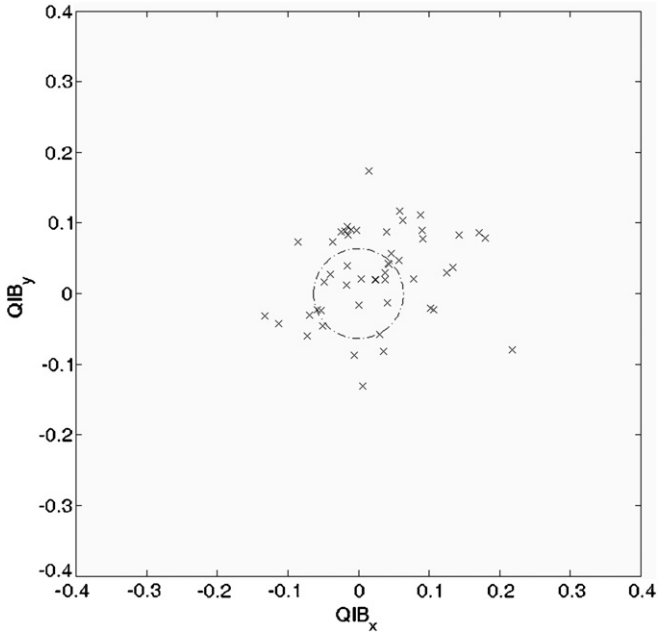

Figure 8. QIB to 50 samples of the previous experiment which was performed by a human operator trying to balance the intensity on the screen. The result shows that 1σ of the QIB for human operated results is about 0.05 in each axis.

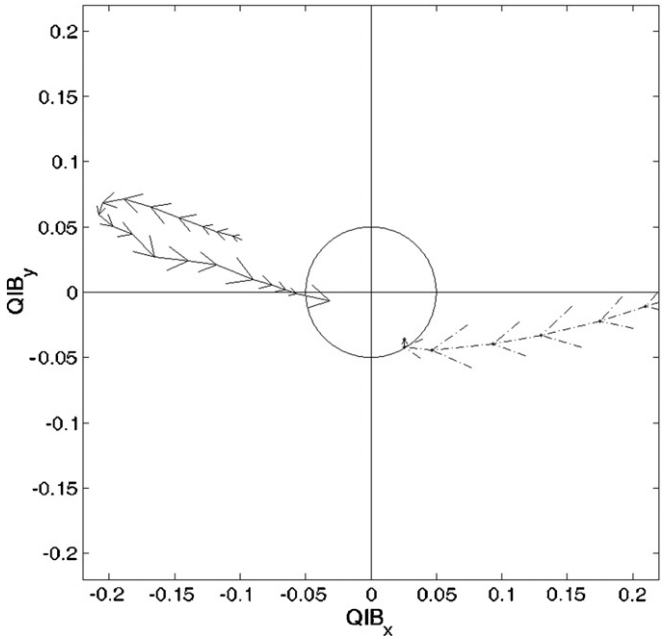

Figure 9. Example of two trajectories of the centering algorithm *L. innocua* sample. The center circle provides the termination criteria for the iterative processing of centering. The left case is when the initial position of centering is displaced more than the radii of the laser beam. The right case shows that of within half a radius of the laser beam.

3.2. Forward scattering

Now we need to understand the relationship between the QIB output and the relative distance between the incident laser beam and the bacterial colony to perform the automated centering process. With the help of the QIB, we have performed one-dimensional scanning of the *L. innocua* colony across the fixed incident laser beam and computed the QIB versus the scanning distance. Figure 7 shows the schematics and result of one-dimensional scanning. As shown in figure 7(*a*), the forward-scattering pattern creates a circularly symmetric pattern as the offset between the center of bacterial colony and the incident Gaussian beam decreases. In one-dimensional scanning of figure 7(*b*), the *x*-axis refers to the physical distance in mm and the *y*-axis reflects the signal output of the QIB_x from the CCD image sensor. Location numbers (1) and (3) refer to when the bacterial colony is barely blocking the incident laser beam such that the QIB_x value is close to the 0 value. When the bacterial colony is further moved to the center of the laser beam, the QIB_x starts to either increase to a positive value or decrease to a negative value. The sign of the QIB_x signal reveals the direction of movement to balance the intensity around the center of the CCD image frame. Location (2) shows the instance when the bacterial colony is centered on the incident laser beam. The corresponding scattering pattern is shown in the right column. We design the system such that when the QIB_x and QIB_y signal is less than a certain threshold value, the image is automatically captured in bitmap format.

During this process, a question arises on how to determine the centeredness of the scattering pattern which satisfies but does not affect the performance of the classification algorithm. To provide the answer, we applied the same QIB computation scheme to the previously recorded scattering patterns which provided positive results in bacterial classification [11, 13]. Fifty forward-scattering patterns of *L. innocua* where the images were manually centered by a human operator are selected and the same QIB is calculated. The QIB resulted in a 1σ error of 0.05 which is shown as a dashed circle in figure 8. This value is equivalent to approximately 0.15–0.2 mm from the scattering center as shown in figure 7(*b*) which provides us a quantitative threshold value to determine whether the forward-scattering pattern satisfies the centeredness criteria.

Figure 9 shows the variation of the QIB_x and QIB_y signal outputs. The solid line trajectory shows the worst case when the bacterial colony barely touches the edge of the incident laser beam. It required 18 steps of movement since the amount of movement to command the linear actuator is determined by the output of the QIB_x and QIB_y values. The displacement of the linear actuator showed a nonlinear relationship due to the characteristics of light scattering of figure 7(*b*). The dash-dotted line case shows when the offset of the computed centroid of the bacterial colony and true center is less than the radius of the colony. This case shows a trajectory moving toward the center location with only seven steps of adjustment. The average time required for the measurement is 9.75 s per colony.

4. Discussions

The colony locator provides both the total number of bacterial colonies and the centroid of the colony location which is critical to perform a subsequent TSP and centering algorithm. The colony locator is realized via segmentation and

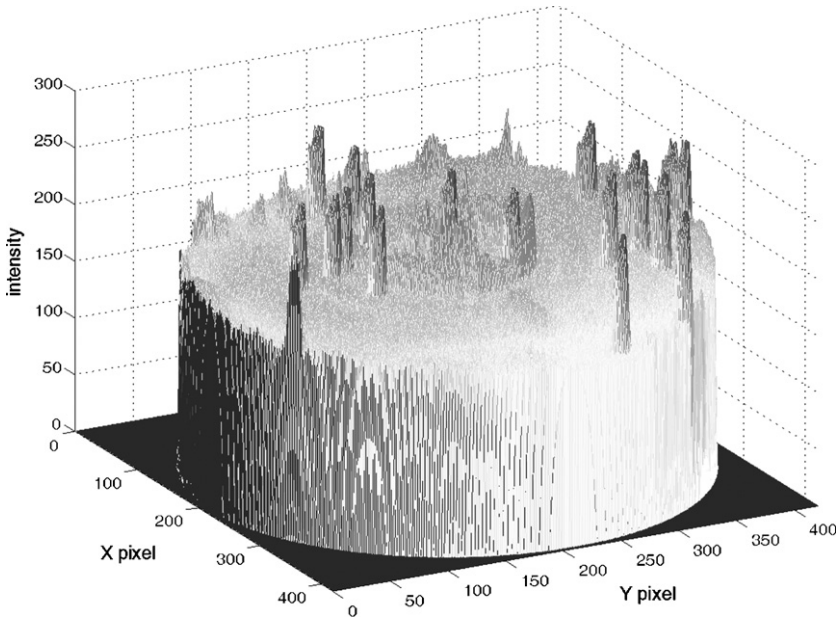

Figure 10. Intensity distribution of the bacterial colony sample. The image provides the 8 bit gray scale intensity of the circular area with a diameter of 400 pixels. The intensity from the reflection of the background (camera, agar, etc) is located around 200 while that of the bacterial colonies is close to 250.

region-growing algorithm. This algorithm is a histogram-based algorithm with further image processing of the binary data set. Therefore, the initial determination of threshold for the binary image which separates the bacterial colony from the surrounding background is the most important process to guarantee the accuracy of colony counting and centroid location of each colony. The threshold of the binary image is determined by analyzing the light intensity distribution captured from the imaging camera. Figure 10 displays the 8 bit gray scale intensity of the circular area of 400 pixel diameter. The intensity distribution provides a quantitative level of the threshold value for accurately capturing the colonies. The circular ring structure is the intensity reflected from the camera while the prominent peaks are the reflected intensity from the bacterial colonies. The trajectory optimization algorithm shows positive results when there is a small number of bacterial colonies. However, the result of the current TSP algorithm shows some limitations when the number of bacterial colonies increases since the TSP algorithm started from a nondeterministic polynomial-time hard (NP hard) problem in computational complexity theory [19], and the overhead for the TSP algorithm computation can offset the reduction of the overall measurement time. In section 3.1, we present the result of CPU time required for the CE and GA methods. Due to their algorithm difference, the CE method required a large amount of time for just solving the optimized trajectory while the GA method provided a similar result within 1 s.

The one-dimensional scanning of figure 7 provides the characteristics of light scattering with the variation of QIB. Since the direction and magnitude of movement of the centering algorithm is determined by the offset of the QIB value, the number of iterative steps required for converging to the centered image depends on the difference between the computed centroid and scattering center. When this difference is greater than the radii of the incident laser beams, the automatic centering process starts the algorithm at the outer interval (32.5–31.7 or 30.2–29.6 mm in figure 7(*b*)). Since the QIB value in this interval is small, the automatic centering algorithm will require multiple steps to translate to the center interval which has a linear relationship between the distance and the QIB value. The initial starting location from the computed centroid determines the offset from the true center location. There can be various error sources that affect the accuracy of the centroid computation such as illumination condition and bacterial colony formation. When this effect is significant the initial starting point of the centering process falls on the outer interval. As shown in figure 9, even this worst case when the initial starting point offset is larger than the radius of the colony size took 4.3 s with 22 iterations to converge to a centered image. The typical case when the initial starting point is offset less than the radius took 1.5 s with seven iterations. Further development of optimizing this process via linearization of the overall distance and QIB value will provide a more robust automatic centering process.

5. Conclusions

Integration and automation for a system that automatically locates the bacterial colony and captures the respective scattering pattern are introduced. The system provides an automatic platform for the identification and classification of a micro-organism which forms a colony on a solid agar surface. The system consists of three major parts: a colony locator, a forward scatterometer and a 2D motion controller. For a colony locator, image segmentation with a region-growing

algorithm is applied to efficiently capture the centroid of the colonies. The Traveling Salesman Problem is solved with CE and GA and concluded that the optimization efficiency is similar but the GA method provided much faster solution compared to the CE method. With the optimization, the total traveling length could be reduced up to 60% depending on the number of bacterial colonies and distributions. QIB is defined to quantitatively compute the degree of centeredness of the forward-scattering pattern, and one-dimensional scan across the fixed incident beam revealed a nonlinear relationship between the distance and the QIB output. The final setup is tested with *L. innocua* sample with an average capture time of 9.75 s per colony.

Acknowledgments

This research was supported through a cooperative agreement with the Agricultural Research Service of the US Department of Agriculture project number 1935-42000-035 and the Center for Food Safety and Engineering at Purdue University.

References

[1] Mukherjee D P, Pal A, Sarma S E and Majumder D D 1995 Bacterial colony counting using distance transform *Int. J. Biomed. Comput.* **38** 131–40

[2] Corkidi G, Diaz-Uribe R, Folch-Mallol J L and Nieto-Sotelo J 1998 COVASIAM: an image analysis method that allows detection of confluent microbial colonies and colonies of various sizes for automated counting *Appl. Environ. Microbiol.* **64** 1400–4

[3] Marotz J, Lübbert C and Eisenbeiß W 2001 Effective object recognition for automated counting of colonies in Petri dishes (automated colony counting) *Comput. Methods Programs Biomed.* **66** 183–98

[4] Bernard R, Kandušer M and Pernuš F 2001 Model-based automated detection of mammalian cell colonies *Phys. Med. Biol.* **46** 3061–72

[5] Barber P R, Vojnovic B, Kelly J, Mayes C R, Boulton P, Woodcock M and Joiner M C 2001 Automated counting of mammalian cells colonies *Phys. Med. Biol.* **46** 63–76

[6] Kawasaki K, Mochizuki A, Matsushita M, Umeda T and Shigesada N 1997 Modeling spatio-temporal pattern generated by *Baccillus Subtilis J. Theor. Biol.* **188** 177–85

[7] Lacasta A M, Cantalapiedra I R, Auguet C E, Peñaranda A and Ramírez-Piscina L 1999 Modeling of spatiotemporal patterns in bacterial colonies *Phys. Rev.* E **59** 7036–41

[8] Mimura M, Sakaguchi H and Matsushita M 2000 Reaction–diffusion modeling of bacterial colony patterns *Physica* A **282** 283–303

[9] Guo S 2004 Optical scattering for bacterial colony detection and characterization *MS Dissertation* Purdue University, West Lafayette, IN

[10] Banada P P, Guo S L, Bayraktar B, Bae E, Rajwa B, Robinson J P, Hirleman E D and Bhunia A K 2007 Optical forward-scattering for detection of *Listeria monocytogenes* and other *Listeria* species *Biosens. Bioelectron.* **22** 1664–71

[11] Bae E, Banada P P, Huff K, Bhunia A K, Robinson J P and Hirleman E D 2007 Biophysical modeling of forward scattering from bacterial colonies using scalar diffraction theory *Appl. Opt.* **46** 3639–48

[12] Bae E, Banada P P, Huff K, Bhunia A K, Robinson J P and Hirleman E D 2008 Analysis of time-resolved scattering from macroscale bacterial colonies *J. Biomed. Opt.* **13** 014010

[13] Bayraktar B, Banada P P, Hirleman E D, Bhunia A K, Robinson J P and Rajwa B 2006 Feature extraction from light-scatter patterns of *Listeria* colonies for identification and classification *J. Biomed. Opt.* **11** 034006

[14] Bhunia A K 2008 Biosensors and bio-based methods for the separation and detection of foodborne pathogens *Adv. Food Nutr. Res.* **54** 1–44

[15] Phillips D 1994 *Image Processing in C* 1st edn (Lawrence, KS: R&D Publication, Inc.)

[16] Mancas M, Gosselin B and Macq B 2005 Segmentation using a region growing thresholding *Proc. Soc. Photo-Opt. Instrum. Eng.* **3448** 340–51

[17] Phan D L, Xu C and Price J 2000 Current methods in medical image segmentation *Ann. Rev. Biomed. Eng.* **2** 315–37

[18] Rubinstein R Y and Kroese D P 2004 *The Cross-Entropy Method: A Unified Approach to Combinatorial Optimization, Monte-Carlo Simulation, and Machine Learning* 1st edn (Berlin: Springer)

[19] Lawler E L, Lenstra J K, Rinnooy Kan A H G and Shmoys D B 1985 *The Traveling Salesman Problem: A Guided Tour of Combinatorial Optimization* 1st edn (New York: Wiley)

[20] Boer P T, Kroese D P, Mannor S and Rubinstein R Y 2003 *A Tutorial on the Cross-Entropy Method* http://iew3.technion.ac.il/CE/tutor.php

[21] Goldberg D E 1989 *Genetic Algorithm in Search, Optimization and Machine Learning* (Reading, MA: Addison-Wesley)

[22] Larranaga P, Kuijpers C M H, Murga R H, Inza I and Dizdarevic S 1999 Genetic algorithms for the Travelling Salesman Problem: a review of representations and operators *Artif. Intell. Rev.* **13** 129–70

[23] Syswerda G 1991 Schedule optimization using genetic algorithms *Handbook of Genetic Algorithms* (Princeton, NJ: Van Nostrand–Reinhold)